

# Autodetachment of diatomic carbon anions from long-lived high-rotation quartet states

Viviane C. Schmidt

*Max-Planck-Institut für Kernphysik, Saupfercheckweg 1, 69117 Heidelberg, Germany*

Roman Čurík\*

*J. Heyrovský Institute of Physical Chemistry, ASCR, Dolejškova 3, 18223 Prague, Czech Republic*

Milan Ončák

*Institut für Ionenphysik und Angewandte Physik,  
Leopold-Franzens-Universität Innsbruck, Technikerstraße 25/3, Innsbruck 6020, Austria*

Klaus Blaum, Sebastian George, Jürgen Göck, Manfred Grieser, Florian Grussie, Robert von Hahn,<sup>†</sup> Claude Krantz, Holger Kreckel, Oldřich Novotný, Kaija Spruck, and Andreas Wolf

*Max-Planck-Institut für Kernphysik, Saupfercheckweg 1, 69117 Heidelberg, Germany*

(Dated: May 13, 2024)

Highly excited  $C_2^-$  ions prominently feature electron detachment at a mean decay time near 3 milliseconds with hitherto unexplained origin. Considering various sources of unimolecular decay, we attribute the signal to the electronic  $C^4\Sigma_u^+$  state. Quartet  $C_2^-$  levels are found to be stabilized against autodetachment by high rotation. Time constants of their rotationally assisted autodetachment into levels opening energetically at lower rotation are calculated by a theory based on the non-local resonance model. For some final levels of significantly less rotation the results conclusively explain the puzzling observations.

Understanding highly excited molecules in the gas phase is vital in fields such as molecular astrophysics [1] and plasma-related surface technology [2]. Especially when they are sputtered from solid surfaces by fast-ion impact [3–6] molecules acquire high rotational and vibrational energy up to the dissociation limit [7]. In competition with their radiative cooling, the excited molecules often show unimolecular decay involving the split-off of electrons or heavy constituents. With molecular anions produced by sputtering and loaded into ion storage rings [8–10], these unimolecular decays were sensitively investigated over storage times up to many seconds [11–14]. Among the studied systems, homonuclear diatomic molecules are particularly interesting as their radiative cooling is strongly suppressed through the absence of a permanent electric dipole moment. Hence, their stability at high internal energy is determined by the unimolecular decay only. For rotationally as well as vibrationally excited states, a unimolecular dissociation was observed in anions such as  $Cu_2^-$  and  $Ag_2^-$ . The process was explained by a tunneling pre-dissociation through the rotational barrier [12]. Moreover, unimolecular electron split-off was detected and attributed to the autodetachment of states with very high vibrational excitation [13, 15]. Ion storage ring experiments thus revealed unanticipated limitations to the long-time stability of small molecules at high internal excitation.

The present work focuses on the stability of highly excited levels in the carbon dimer anion  $C_2^-$ , where the excitation conditions are fundamentally different. The  $C_2^-$  anion is well known [16–22] to have several valence-

excited electronic states that lead to radiative cooling of all vibrational levels except (in the limit of low rotations) the three lowest levels. Hence, radiative quenching of vibrational excitation competes with the unimolecular decay. Nevertheless, such decay was observed on millisecond to second timescales by several ion storage ring experiments [22–25]. Electron split-off from  $C_2^-$  is observed with near-exponential decay at a time constant close to 3 ms which could not be linked to those expected for the competing radiative decay [22, 24]. Aside from speculations, discussed below, no explanation could so far be given for the mechanism behind these observations. We show here that theoretical understanding of the electron split-off from rotating molecules yields a basis to explain these mysterious signals.

Electron detachment from excited  $C_2^-$  can be caused by vibrational autodetachment (AD). The process was observed by electron spectroscopy [19, 20] starting from the  $X^2\Sigma_g^+$  ground state of  $C_2^-$ . Resonances of the electron spectra were assigned to AD from levels in the valence-excited states  $B^2\Sigma_u^+$  (vibrational quantum number  $v \geq 5$ ) or (less often)  $A^2\Pi_u$ . From their widths, AD lifetimes of  $\lesssim 10^{-8}$  s could be determined. The excitation energy required for AD is given by the  $C_2^-$  detachment threshold (3.269 eV [26]). Taking into account also radiative decay [21], all  $B^2\Sigma_u^+$  levels are expected to live for  $< 0.1 \mu\text{s}$  and can be eliminated as a source of the stored-beam  $C_2^-$  AD signal. For AD from levels in the  $X^2\Sigma_g^+$  and  $A^2\Pi_u$  states of  $C_2^-$ , high vibrational excitation ( $v \geq 16$  [26]) is necessary and the processes were hardly observable so far. As a source of

the unimolecular electron split-off signal from stored  $C_2^-$  beams, they become unlikely as they would require extremely high vibrational temperature in view of the high detachment threshold. At this point, the theoretically predicted [27, 28] lowest quartet state of  $C_2^-$ ,  $C^4\Sigma_u^+$ , enters as a further possible source of the stored-beam  $C_2^-$  AD signal. In contrast to the anionic doublet states, the  $C^4\Sigma_u^+$  electronic energy lies  $\sim 1.4$  eV above those of the lowest two neutral states of  $C_2$ ,  $X^1\Sigma_g^+$  and  $A^3\Pi_u$ , at the equilibrium internuclear distance of  $C_2^-$ . Hence, the anionic quartet states are expected to be highly unstable against AD with pico- to femtosecond lifetimes. To our knowledge, no experimental information on this state is available and its role in AD processes from  $C_2^-$  was considered only speculatively up to now [22, 24].

Here we theoretically address the stability against AD for levels in the  $C^4\Sigma_u^+$  electronic state of  $C_2^-$  and show that rotational excitation strongly influences their AD decay. Since the energy balance of AD significantly depends on changes in the rotational excitation during this process, we are led to consider a mechanism that we name “rotationally assisted” AD. While some investigations on the stability of rotating anions were performed earlier [29–31], a method to describe rotationally assisted AD is not at hand. We extend an approach applied in previous anion stability studies. It explicitly allows for electronically unstable initial anion states of resonant character, using a diabatic representation and employing the non-local resonance model [32, 33]. This method fundamentally differs from that appropriate to the AD rates from doublet  $C_2^-$  [19], based on non-adiabatic perturbation of adiabatic molecular levels as introduced by Berry [34].

We find that  $C_2^-$  ions in the  $C^4\Sigma_u^+$  state become stable with  $\gtrsim 1$  ms lifetimes at strong molecular rotation. Within the accuracy of the ab-initio predictions, a model based on the calculated AD rates can explain the temporal behaviour of the electron split-off signal observed at ion storage rings. In a companion paper (CP) [35] we present experimental results on unimolecular electron split-off (AD) as well as dissociation (autofragmentation, AF) using  $C_2^-$  ions in a cryogenic ion storage ring. Moreover, we develop a detailed model of  $C_2^-$  at high rotational and vibrational excitation that includes the radiative decay as well as the AD and AF rates for all relevant levels in the  $X^2\Sigma_g^+$ ,  $A^2\Pi_u$  and  $C^4\Sigma_u^+$  states. Together with a model of the level populations, these data complement the rates of rotationally assisted AD calculated here and allow us to show that AD and AF from  $C^4\Sigma_u^+$   $C_2^-$  ions can plausibly explain the observed signals in their intensities and their temporal behaviour. Below, we shortly summarize the experimental AD signal and then present our theoretical method to assess the stability and the rotationally assisted AD decay of quartet  $C_2^-$ .

The count rates of particles split-off from a stored  $C_2^-$  beam following its injection into a storage ring are shown

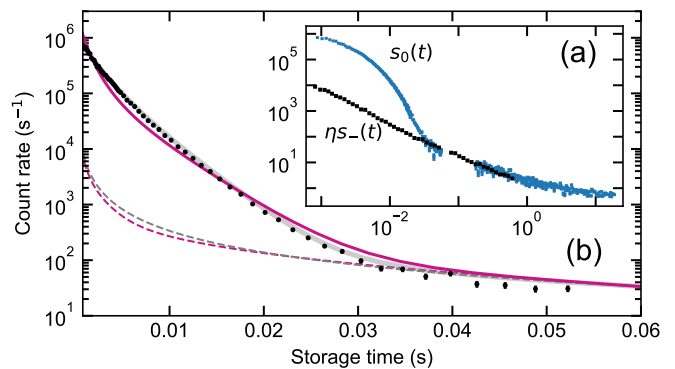


FIG. 1. Count rates by electron split-off (AD) and dissociation (AF) from  $C_2^-$  as functions of the storage time  $t$  [35]. (a) Signals  $s_0$  and  $\eta s_-$  (see the text) with  $\eta = 0.75$ . (b) Neutral signal  $s_0$ , assigned to AD and AF, with data shown as symbols. Thick grey line: fit for bi-exponential time dependence of the AD signal, assuming a background (dashed line) from AF varying as  $\propto t^c$  with  $c = -1.287$  as a fit to  $\eta s_-$  at  $t < 0.06$  s in (a). Purple lines: sum  $s_d + \eta s_f$  of modeled AD and AF rates from  $C_2^-$  ions in the  $C^4\Sigma_u^+$  state (full line) and the modeled AF background  $\eta s_f$  (dashed).

in Fig. 1. These data were obtained at the cryogenic storage ring CSR at the Max Planck Institute for Nuclear Physics in Heidelberg, Germany, as described in the CP [35]. The ions are produced in a sputter ion source and accelerated to 60 keV. A number of about  $4 \times 10^7$  stored ions is derived from the injected beam current. Products of unimolecular decay are separated from the stored beam at the deflectors of the storage ring by their differing charge-to-mass ratios. A single counting detector behind one of the deflectors was used and in separate runs placed to intersect neutral fragments ( $C_2$  or  $C$ , count rate  $s_0$ ) or  $C^-$  fragments ( $s_-$ ). Products from electron split-off (AD) contribute to  $s_0$  only, while each dissociation event (AF) contributes to  $s_0$  and  $s_-$ . The cryogenic cooling of the storage ring leads to extreme vacuum such that  $C_2^-$  destruction in collisions with residual gas molecules occurs too rarely to contribute significantly to the rates. Also, ion loss from the stored beam is insignificant during the displayed storage time interval.

The neutral rate  $s_0$  shows a strong initial peak not appearing in  $s_-$ , thus corresponding to the AD signature. The temporal dependence of this AD component is close to exponential, consistent with the time constant near 3 ms observed earlier [22, 24]. We extract the AD component as  $s_0 - \eta s_-$  with a near-unity factor  $\eta$  compensating intensity fluctuations between the runs [35]. A fit to this component shows that a bi-exponential decay with time constants  $\tau_1 = 3.31(4)$  ms and  $\tau_2 = 1.56(5)$  ms describes the data well.

The complete picture of coexistent decay processes by AD, AF, and radiative relaxation is discussed in the CP [35]. It turns out that for levels showing AD decay, decay

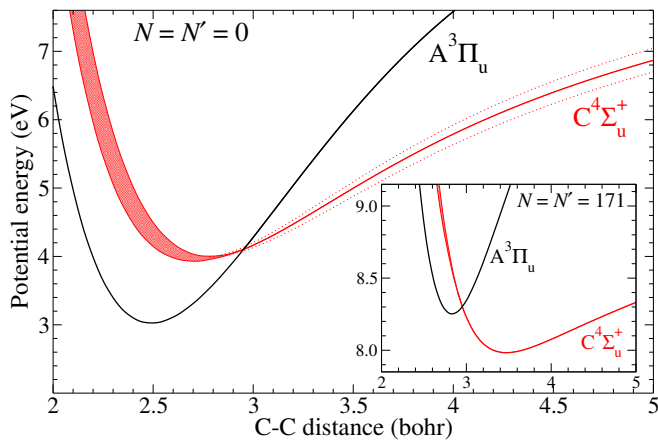


FIG. 2. AD from  $C_2^-(C^4\Sigma_u)$ . Black line:  $A^3\Pi_u$  neutral potential curve; red: potential of the  $C^4\Sigma_u$  anionic resonance curve with the vertical spread showing the  $R$ -dependent width of the state in the AD region. Inset: rearrangement of the curves for the exemplary nuclear rotation quantum numbers  $N = N' = 171$ . The zero of the energy scale is set to the rovibrational ground state of  $C_2^-(C^2\Sigma_g^+)$ .

by AF is mostly negligible. Moreover, in contrast to AF, radiative decay is typically not significant in combination with AD decay. The decay constant of the AD signal can therefore be considered to be close to that for the AD process itself, as determined by the theory. Accordingly, the time constants  $\tau_1, \tau_2$  are used as indicative of the experimental results in the comparison below.

Excluding the bound  $C_2^-$  doublet states, another candidate is the lowest quartet state  $C^4\Sigma_u^+$ . Situated above the detachment limit, it can decay by spin-allowed AD into  $C_2(A^3\Pi_u)$ . While predicted in multiple theoretical studies [27, 28, 36–38] it could never be unambiguously assigned to any measured feature [22, 39]. For the present work, *ab initio* calculations were performed [35] using the MOLPRO package [40] to consistently locate this and the three lower lying anionic states together with the first two neutral states of  $C_2$ . Rotationless potential energy curves of the  $C^4\Sigma_u^+$  anionic and the  $A^3\Pi_u$  neutral states are shown as a function of the internuclear distance  $R$  in Fig. 2. For some  $R$  range,  $C_2^-(C^4\Sigma_u^+)$  lies above  $C_2(A^3\Pi_u)$ , with the indicated resonance widths  $\Gamma_{\text{eq}} = 0.48$  eV. In the absence of nuclear rotation, such resonance widths enable very fast AD on atomic time scales [38]. For the bound state part of the anion’s curve ( $R > 3$  a.u.) we consider *ab-initio* calculations with uncertainties of  $\pm 170$  meV at  $R = 5$  a.u. shown by the dotted lines in Fig. 2 and described in the Supplemental Material (SM)[41].

The arrangement of the curves changes for high rotations. Starting at the  $C_2^-$  nuclear rotation with quantum number  $N = 155$ , the zero-point energy (ZPE) of the  $C^4\Sigma_u^+$  curve lies below the ZPE of the  $A^3\Pi_u$  curve for the  $C_2$  nuclear rotation  $N' = N$  [35]. Here, the ZPE refers

to the energy of the lowest vibrational level ( $v = 0$ ) in the potentials. This form of rearrangement of the neutral and anion curves for the higher rotational states was previously documented for  $N=20-40$  of the  $H_2^-$  and  $D_2^-$  ions [29, 31, 42]. For the present, heavier molecular system, a similar rearrangement is reached for much higher rotational states in order to offset smaller rotational constants. E.g. for  $N = 171$  (see Fig. 2), the ZPE of the quartet state lies clearly below that of the neutral triplet state for  $N' = N$ . This suggests that AD is suppressed for some vibrational levels in  $C_2^-(C^4\Sigma_u^+, N = 171)$ . Moreover,  $C_2^-$  vibrational levels appearing bound for  $N' = N$  for energetic reasons are in fact not absolutely stable against AD considering processes with  $N' < N$ , in particular at higher values of  $|N' - N|$ .

A theory describing rotationally assisted AD of  $C_2^-$  requires a combination of two approaches. The first one was used to predict long-lived anion states of  $H_2^-$  (and its isotopologues) [29, 31]. However, the technique used in these studies did not allow for a change of the electronic angular momentum  $l$  and kept it fixed in the  $p$  wave. When applied to the present case, such limited rotational change of the molecular frame during the AD process predicts lifetimes shorter than  $10^{-10}$  s for the  $C^4\Sigma_u^+$  levels. The second step corrects these shortcomings by incorporating the rotational degrees of freedom into the non-local resonance model [32]. Its derivation for  $\Sigma$ -states of anion and neutral can be found in Ref. [43]. A similar procedure, based on the local complex potential was developed for the description of the angular distributions of the molecular fragments resulting from the dissociative electron attachment process [44].

Here we adopt a theory that is an extension of the work by Čížek et al. [29–31, 43]. For the non-dissociative states  $|\Phi\rangle$  and the narrow resonances, the diagonalization of the effective complex Hamiltonian  $H^{\text{eff}}$  provides the resonance energy  $E$  as

$$H^{\text{eff}}(E)|\Phi\rangle = E|\Phi\rangle. \quad (1)$$

The energy dependence of  $H^{\text{eff}}$  leads to an iterative procedure that usually converged within a few iterations in the present study. The effective nuclear Hamiltonian  $H^{\text{eff}}$  plays a primary role in projection-operator methods that have been previously used to study the AD [29, 30], dissociative electron attachment [44–47], vibrational excitation [48–50], and associative detachment [51, 52]. In its local form it can be written, for each of the initial anion’s rotation states  $N$ , as [41]

$$H_N^{\text{eff}} = T + \frac{N(N+1)}{2\mu R^2} + V_r(R) - \frac{i}{2}\Gamma_N(R). \quad (2)$$

Here  $T$  is the radial nuclear kinetic energy operator,  $V_r(R)$  is the real part of the anion’s potential, and  $\Gamma_N(R)$

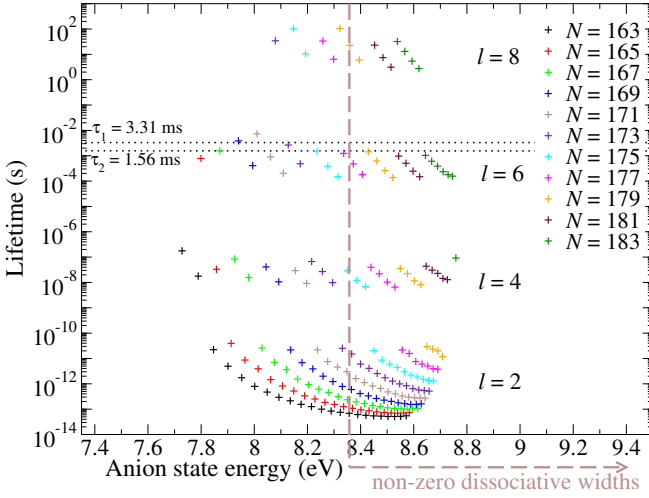


FIG. 3. Lifetimes of the anion states for the different anion rotational quantum numbers  $N$ , including the electron partial wave  $l$  and the threshold for tunneling predissociation (dashed line). The dotted horizontal lines depict the lifetimes  $\tau_1$  and  $\tau_2$  determined from the fit of the present experimental data.

is the  $R$ -dependent total width [41]

$$\Gamma_N(R) = \sum_{lN'\nu'\eta'} g_{lN'N}^{\eta'} (2N' + 1) \begin{pmatrix} l & N' & N \\ \Lambda & -\Lambda & 0 \end{pmatrix}^2 \times \Gamma_l(R) |\chi_{\nu'N'}(R)|^2, \quad (3)$$

where  $\Gamma_l(R)$  is the local partial width,  $\chi_{\nu'N'}(R)$  are the final rovibrational states of the neutral molecule, and the factor  $g_{lN'N}^{\eta'} = 0$  or  $1$  is selecting only one of the 2 final, nearly degenerate  $A^3\Pi_u$  states (hence  $\Lambda = 1$ ) in order to preserve the nuclear spin state during the AD process [41]. The imaginary part (3) of the  $H^{\text{eff}}$  (2) clearly shows how the lifetime of the initial anion state ( $C^4\Sigma_u^+, N$ ) is determined by the final neutral state ( $\nu'N'$ ) and by the rate at which the electron is ejected in the partial wave  $l$ , the rate defined by the partial width  $\Gamma_l$ .

Both the initial and the final states are treated as Hund's case (b). The splitting of the final  $A^3\Pi_u$  states due to the  $\Lambda$ -doubling is  $< 3$  meV up to  $N' = 180$  [53] and it is neglected in the present study.

Calculated lifetimes for a number of initial  $N$  states are shown in Fig. 3. Evidently, the lifetimes of anion states with the same  $N$  spread over many orders of magnitude, as has been similarly seen for the  $H_2^-$  calculations [29]. Furthermore, the spectrum can be organized into well-separated groups with lifetimes similar on the logarithmic scale. Closer inspection reveals that the states in each group also share the lowest angular momentum  $l$  of the ejected electron. The discussion of the lifetimes follows:

(i) Sufficiently long lifetimes of the order of  $10^{-3}$  s are only available for an interval of initial rotational states  $N = 165 - 183$ . For the lower initial rotational states

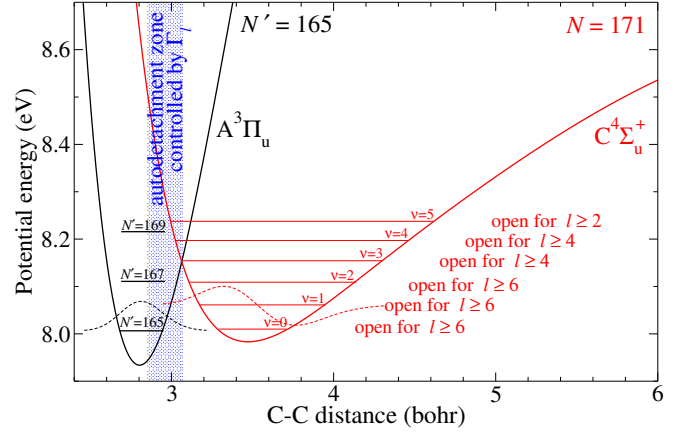


FIG. 4. Potential curves for the AD process from the  $N = 171$  anion states. Neutral ZPE levels are shown for rotational quanta  $N' = 165, 167, 169$ . The lowest angular momentum  $l$  of the ejected electron is assigned to the first 6 anionic states supported by the  $C_2^-$  ( $C^4\Sigma_u^+, N = 171$ ) state.

the rearrangement effect is not strong enough to forbid the faster AD process through  $l = 2, 4$  partial waves controlled by the corresponding partial widths  $\Gamma_l$  (see the SM [41], Sec. II). On the other side, the initial states with  $N > 183$  are dissociative. The dissociation threshold is displayed in Fig. 3.

(ii) Fig. 4 shows that the neutral and anionic curves rearrange such that only the tail of the anionic vibrational function is available for the AD. The example illustrates cases for some  $v$  where  $\Delta N = |N' - N|$  must be as high as 6 for AD becoming energetically possible. The AD rate is then primarily controlled by the partial width  $\Gamma_6$ . Its value is suppressed by the threshold law  $\Gamma_l(E) \sim E^{l+1/2}$  [32] in the AD zone, resulting in millisecond AD lifetimes for the  $v = 0, 1, 2$  states of  $C_2^-$  ( $C^4\Sigma_u^+, N = 171$ ).

In Fig. 3 the observed decay times  $\tau_1$  and  $\tau_2$  are compared to the calculated  $\tau_{\text{AD}}(v, N)$ . The group of several states corresponding to the angular momentum  $l = 6$  of the ejected electron qualifies as the origin of the observed decay. The time constants  $\tau_{\text{AD}}(v, N)$  are implemented in the  $C_2^-$  unimolecular decay model of the CP [35], yielding modeled signals  $s_d(t)$  for AD and  $s_f(t)$  for AF. When the excitation temperatures of the ion beam are set according to available evidence on sputter ion sources, respecting an upper limit of  $1 \times 10^4$  K even for thermal tails of the rotational and vibrational population distributions, the  $C^4\Sigma_u^+$  levels turn out to be the only ones able to yield the observed AD signals. The set of  $\tau_{\text{AD}}(v, N)$  determines the temporal trend. No significant further decay is found, although the model includes all decay paths. The count rates in the AD signal are reproduced when the population fraction of all  $C^4\Sigma_u^+ C_2^-$  anions with AD lifetimes of  $> 10^{-6}$  s is set to  $6 \times 10^{-3}$ .

Intensity and temporal shape of the AD signal can be

well modeled within the given uncertainty of the ab-initio  $C^4\Sigma_u^+$  potential  $V(R)$ . Closest agreement, as shown in Fig. 1(b), is reached when the potential at  $R = 5$  a.u. is increased to the upper margin. As shown in the CP [35], the decay becomes slower with  $V(R)$  chosen in other regions of the uncertainty range. The model also shows that, for the same population distribution [35], the AF signal ( $s_-$ ) stems from rotationally stabilized  $C_2^-$  quartet levels with highest rotation. Accordingly, the modeled signals  $s_f$  and  $s_d + \eta s_f$  are shown in Fig. 1(b), where  $s_d$  largely dominates the neutral signal  $s_0$ .

Using the model, we have also probed the excitation conditions of the  $C_2^-$  beam which could explain the observed AD and AF signals without a quartet  $C_2^-$  population. Here, substantial thermal tails (carrying 3.5–5% of the population) with temperatures of  $3 \times 10^4$  K are required. We consider such a scenario highly unlikely and see strong evidence for the presence of quartet levels in the investigated  $C_2^-$  ion beams.

In summary, we present a theory that predicts the AD of a diatomic molecule when it is connected with changes of rotation by as many as six quanta. The correspondingly long AD lifetimes become relevant for rotationally stabilized quartet levels of the  $C_2^-$  anion and reproduce the AD signals with long decay times on stored ensembles of this anion observed in puzzling observations over recent years.

This article comprises parts of the doctoral thesis of V.C.S. to be submitted at the Ruprecht-Karls-Universität Heidelberg, Germany. The work of R.Č. has been supported by the Czech Science Foundation (Grant No. GACR 21-12598S). Financial support by the Max Planck Society is acknowledged. The computational results presented have been in part achieved using the HPC infrastructure LEO of the University of Innsbruck.

---

\* roman.curik@jh-inst.cas.cz

† Deceased

- [1] A. G. G. M. Tielens, The molecular universe, *Rev. Mod. Phys.* **85**, 1021 (2013).
- [2] G. S. Oehrlein and S. Hamaguchi, Foundations of low-temperature plasma enhanced materials synthesis and etching, *Plasma Sources Sci. Technol.* **27**, 023001 (2018).
- [3] H. M. Urbassek, Sputtering of molecules, *Nucl. Instrum. Methods Phys. Res. B* **18**, 587 (1986).
- [4] C. Anders, R. Pedrys, and H. M. Urbassek, Molecule emission from condensed Ar and O<sub>2</sub> targets by 750 eV Ne impact, *Nucl. Instrum. Methods Phys. Res. B* **352**, 195 (2015).
- [5] E. A. Muntean, P. Lacerda, T. A. Field, A. Fitzsimmons, W. C. Fraser, A. C. Hunniford, and R. W. McCullough, A laboratory study of water ice erosion by low-energy ions, *Mon. Not. R. Astron. Soc.* **462**, 3361 (2016).
- [6] C. Arnas, C. Dominique, P. Roubin, C. Martin, C. Brosset, and B. Pégourié, Characterisation of carbon dust produced in sputtering discharges and in the Tore Supra tokamak, *J. Nucl. Mater.* **353**, 80 (2006).
- [7] C. Anders, R. Pedrys, and H. M. Urbassek, Atom and molecule emission caused by ion impact into a frozen oxygen target: Role of rovibrational excitation, *Nucl. Instrum. Methods Phys. Res. B* **315**, 308 (2013).
- [8] R. von Hahn, A. Becker, F. Berg, K. Blaum, C. Breitenfeldt, H. Fadil, F. Fellenberger, M. Froese, S. George, J. Göck, M. Grieser, F. Grussie, E. A. Guerin, O. Heber, P. Herwig, J. Karthein, C. Krantz, H. Kreckel, M. Lange, F. Laux, S. Lohmann, S. Menk, C. Meyer, P. M. Mishra, O. Novotný, A. P. O'Connor, D. A. Orlov, M. L. Rappaport, R. Repnow, S. Saurabh, S. Schippers, C. D. Schröter, D. Schwalm, L. Schweikhard, T. Sieber, A. Shornikov, K. Spruck, S. Sunil Kumar, J. Ullrich, X. Urbain, S. Vogel, P. Wilhelm, A. Wolf, and D. Zajfman, The cryogenic storage ring CSR, *Rev. Sci. Instrum.* **87**, 063115 (2016).
- [9] H. T. Schmidt, R. D. Thomas, M. Gatchell, S. Rosén, P. Reinhed, P. Löfgren, L. Brännholm, M. Blom, M. Björkhage, E. Bäckström, J. D. Alexander, S. Leontein, D. Hanstorp, H. Zettergren, L. Liljeby, A. Källberg, A. Simonsson, F. Hellberg, S. Mannervik, M. Larsson, W. D. Geppert, K. G. Rensfelt, H. Danared, A. Paál, M. Masuda, P. Halldén, G. Andler, M. H. Stockett, T. Chen, G. Källersjö, J. Weimer, K. Hansen, H. Hartman, and H. Cederquist, First storage of ion beams in the Double Electrostatic Ion-Ring Experiment: DESIREE, *Rev. Sci. Instrum.* **84**, 055115 (2013).
- [10] H. T. Schmidt, S. Rosén, R. D. Thomas, M. H. Stockett, W. D. Geppert, A. Larson, P. Löfgren, A. Simonsson, A. Källberg, P. Reinhed, M. Björkhage, M. Blom, J. D. Alexander, P. K. Najeeb, M. Ji, N. Kono, E. K. Anderson, G. Eklund, M. K. Kristiansson, O. M. Hole, D. Hanstorp, H. Hartman, P. S. Barklem, J. Grumer, K. Hansen, M. Gatchell, H. Cederquist, and H. Zettergren, Negative ion relaxation and reactions in a cryogenic storage ring, *J. Phys.: Conf. Ser.* **1412**, 062006 (2020).
- [11] S. Menk, S. Das, K. Blaum, M. W. Froese, M. Lange, M. Mukherjee, R. Repnow, D. Schwalm, R. von Hahn, and A. Wolf, Vibrational autodetachment of sulfur hexafluoride anions at its long-lifetime limit, *Phys. Rev. A* **89**, 022502 (2014).
- [12] J. Fedor, K. Hansen, J. U. Andersen, and P. Hvelplund, Nonthermal power law decay of metal dimer anions, *Phys. Rev. Lett.* **94**, 113201 (2005).
- [13] E. K. Anderson, A. F. Schmidt-May, P. K. Najeeb, G. Eklund, K. C. Chartkunchand, S. Rosén, Å. Larson, K. Hansen, H. Cederquist, H. Zettergren, and H. T. Schmidt, Spontaneous electron emission from hot silver dimer anions: Breakdown of the Born–Oppenheimer approximation, *Phys. Rev. Lett.* **124**, 173001 (2020).
- [14] S. Iida, S. Kuma, H. Tanuma, T. Azuma, and H. Shimomaru, State-selective observation of radiative cooling of vibrationally excited  $C_2^-$ , *J. Phys. Chem. Lett.* **11**, 10526 (2020); Correction to "State-selective observation of radiative cooling of vibrationally excited  $C_2^-$ ", *J. Phys. Chem. Lett.* **12**, 8980 (2021).
- [15] P. Jasik, J. Franz, D. Kedziera, T. Kilich, J. Kozicki, and J. E. Sienkiewicz, Spontaneous electron emission vs dissociation in internally hot silver dimer anions, *J. Chem. Phys.* **154**, 164301 (2021).
- [16] G. Herzberg and A. Lagerqvist, A new spectrum associated with diatomic carbon, *Can. J. Phys.* **46**, 2363 (1968).

- [17] W. Lineberger and T. Patterson, Two photon photodetachment spectroscopy: The  $C_2^-$   $^2\sigma$  states, *Chem. Phys. Lett.* **13**, 40 (1972).
- [18] D. E. Milligan and M. E. Jacox, Studies of the photoproduction of electrons in inert solid matrices. the electronic spectrum of the species  $C_2^-$ , *J. Chem. Phys.* **51**, 1952 (1969).
- [19] R. Mead, U. Hefter, P. Schulz, and W. Lineberger, Ultrahigh resolution spectroscopy of  $C_2^-$ : The A  $^2\Pi_u$  state characterized by deperturbation methods, *J. Chem. Phys.* **82**, 1723 (1985).
- [20] U. Hefter, R. D. Mead, P. A. Schulz, and W. C. Lineberger, Ultrahigh-resolution study of autodetachment in  $C_2^-$ , *Phys. Rev. A* **28**, 1429 (1983).
- [21] P. Rosmus and H. Werner, Multireference-CI calculations of radiative transition probabilities in  $C_2^-$ , *J. Chem. Phys.* **80**, 5085 (1984).
- [22] H. B. Pedersen, C. Brink, L. H. Andersen, N. Bjerre, P. Hvelplund, D. Kella, and H. Shen, Experimental investigation of radiative lifetimes of vibrational levels at the electronic ground state of  $C_2^-$ , *J. Chem. Phys.* **109**, 5849 (1998).
- [23] J. U. Andersen, C. Brink, P. Hvelplund, M. O. Larsson, and H. Shen, Carbon clusters in a storage ring, *Z. Phys. D* **40**, 365 (1997).
- [24] M. Iizawa, S. Kuma, N. Kimura, K. Chartkunchand, S. Harayama, T. Azuma, and Y. Nakano, Photodetachment spectroscopy of highly excited  $C_2^-$  and their temporal evolution in the ion storage ring RICE, *J. Phys. Soc. Jpn.* **91**, 084302 (2022).
- [25] Preliminary results on autofragmentation and autodetachment from  $C_2^-$  presented by N. Kono, R. Paul, M. Gatchell, H. Zettergren and H. T. Schmidt at the Working-Group 1 and Working-Group 2 Conference of the COST action MD-GAS, March 15–19, 2021.
- [26] K. Ervin and W. Lineberger, Photoelectron spectra of  $C_2^-$  and  $C_2H^-$ , *J. Phys. Chem.* **95**, 1167 (1991).
- [27] P. W. Thulstrup and E. W. Thulstrup, A theoretical investigation of the low-lying states of the  $C_2^-$  ion, *Chem. Phys. Lett.* **26**, 144 (1974).
- [28] W. Shi, C. Li, H. Meng, J. Wei, L. Deng, and C. Yang, Ab initio study of the low-lying electronic states of the  $C_2^-$  anion, *Comput. Theor. Chem.* **1079**, 57 (2016).
- [29] R. Golser, H. Gnaser, W. Kutschera, A. Priller, P. Steier, A. Wallner, M. Čížek, J. Horáček, and W. Domcke, Experimental and theoretical evidence for long-lived molecular hydrogen anions  $H_2^-$  and  $D_2^-$ , *Phys. Rev. Lett.* **94**, 223003 (2005).
- [30] M. Čížek, J. Horáček, and W. Domcke, Long-lived anionic states of  $H_2$ , HD,  $D_2$ , and  $T_2$ , *Phys. Rev. A* **75**, 012507 (2007).
- [31] R. Marion, M. Čížek, and X. Urbain, Autodetachment spectroscopy of metastable  $D_2^-$  and  $HD^-$ , *Phys. Rev. A* **107**, 052808 (2023).
- [32] W. Domcke, Theory of resonance and threshold effects in electron-molecule collisions: The projection-operator approach, *Phys. Rep.* **208**, 97 (1991).
- [33] M. Čížek, J. Horáček, and W. Domcke, Nuclear dynamics of the H collision complex beyond the local approximation: associative detachment and dissociative attachment to rotationally and vibrationally excited molecules, *J. Phys. B: Atom. Molec. Phys.* **31**, 2571 (1998).
- [34] R. S. Berry, Ionization of molecules at low energies, *J. Chem. Phys.* **45**, 1228 (1966).
- [35] V. C. Schmidt, R. Čurík, M. Ončák, K. Blaum, S. George, J. Göck, M. Grieser, F. Grussie, R. von Hahn, C. Krantz, H. Kreckel, O. Novotný, K. Spruck, and A. Wolf, Unimolecular processes in diatomic carbon anions at high rotational excitation, Companion paper to be submitted to *Phys. Rev. A*.
- [36] J. Barsuhn, Nonempirical calculations on the electronic spectrum of the molecular ion  $C_2^-$ , *J. Phys. B: Atom. Molec. Phys.* **7**, 155 (1974).
- [37] M. Zeitz, S. D. Peyerimhoff, and R. J. Buenker, A theoretical study of the bound electronic states of the  $C_2$  negative ion, *Chem. Phys. Lett.* **64**, 243 (1979).
- [38] G. Halmová, J. D. Gorfinkiel, and J. Tennyson, Low-energy electron collisions with  $C_2$  using the R-matrix method, *J. Phys. B: Atom. Molec. Phys.* **39**, 2849 (2006).
- [39] A. Naaman, K. G. Bhushan, H. B. Pedersen, N. Altstein, O. Heber, M. L. Rappaport, R. Moalem, and D. Zajfman, Metastable states of negative carbon clusters:  $C_n^-$ ,  $n = 2-6$ , *J. Chem. Phys.* **113**, 4662 (2000).
- [40] H. J. Werner, P. J. Knowles, R. Lindh, F. R. Knizia, F. R. Manby, M. Schütz, and Others, MOLPRO, version 2012.1, a package of ab initio programs (2012).
- [41] Supplemental Material containing details for the derivation of the  $f(e)$  operator for multiple electronic partial waves and for the electronic  $\pi$  states of the final neutral molecule.
- [42] B. Jordon-Thaden, H. Kreckel, R. Golser, D. Schwalm, M. H. Berg, H. Buhr, H. Gnaser, M. Grieser, O. Heber, M. Lange, O. Novotný, S. Novotny, H. B. Pedersen, A. Petrigiani, R. Repnow, H. Rubinstein, D. Shafir, A. Wolf, and D. Zajfman, Structure and Stability of the Negative Hydrogen Molecular Ion, *Phys. Rev. Lett.* **107**, 193003 (2011).
- [43] M. Čížek and K. Houfek, Nonlocal theory of resonance electron-molecule scattering, in *Low-energy electron scattering from molecules, biomolecules and surfaces*, edited by P. Čársky and R. Čurík (CRC Press, Boca Raton, 2012) 1st ed., Chap. 4, pp. 91–125.
- [44] D. J. Haxton, C. W. McCurdy, and T. N. Rescigno, Angular dependence of dissociative electron attachment to polyatomic molecules: Application to the  $^2B_1$  metastable state of the  $H_2O$  and  $H_2S$  anions, *Phys. Rev. A* **73**, 062724 (2006).
- [45] K. Houfek, M. Čížek, and J. Horáček, Calculation of rate constants for dissociative attachment of low-energy electrons to hydrogen halides HCl, HBr, and HI and their deuterated analogs, *Phys. Rev. A* **66**, 062702 (2002).
- [46] H. Hotop, M. Ruf, M. Allan, and I. I. Fabrikant, Resonance and threshold phenomena in low-energy electron collisions with molecules and clusters, *Adv. At. Mol. Opt. Phys.* **49**, 85 (2003).
- [47] M. Zawadzki, M. Čížek, K. Houfek, R. Čurík, M. Ferus, S. Civiš, J. Kočíšek, and J. Fedor, Resonances and dissociative electron attachment in HNCO, *Phys. Rev. Lett.* **121**, 143402 (2018).
- [48] T. N. Rescigno, W. A. Isaacs, A. E. Orel, H.-D. Meyer, and C. W. McCurdy, Theoretical study of resonant vibrational excitation of  $CO_2$  by electron impact, *Phys. Rev. A* **65**, 032716 (2002).
- [49] M. Čížek, J. Horáček, M. Allan, I. I. Fabrikant, and W. Domcke, Vibrational excitation of hydrogen fluoride by low-energy electrons: theory and experiment, *J. Phys. B: At. Mol. Opt. Phys.* **36**, 2837 (2003).
- [50] T. P. Ragesh Kumar, P. Nag, M. Ranković, R. Čurík,

- A. Knížek, S. Civiš, M. Ferus, J. Trnka, K. Houfek, M. Čížek, and J. Fedor, Electron-impact vibrational excitation of isocyanic acid HNCO, *Phys. Rev. A* **102**, 062822 (2020).
- [51] K. A. Miller, H. Bruhns, M. Čížek, J. Eliášek, R. Cabrera-Trujillo, H. Kreckel, A. P. O'Connor, X. Urbain, and D. W. Savin, Isotope effect for associative detachment:  $\text{H}(\text{D})^- + \text{H}(\text{D}) \rightarrow \text{H}_2(\text{D}_2) + e^-$ , *Phys. Rev. A* **86**, 032714 (2012).
- [52] Š. Roučka, D. Mulin, P. Jusko, M. Čížek, J. Eliášek, R. Plašil, D. Gerlich, and J. Glosík, Electron transfer and associative detachment in low-temperature collisions of  $\text{D}^-$  with H, *J. Phys. Chem. Lett.* **6**, 4762 (2015).
- [53] M. C. Curtis and P. J. Sarre, High-resolution laser spectroscopy of the Swan system ( $d^3\Pi_g-a^3\Pi_u$ ) of  $\text{C}_2$  in an organic halide-alkali metal flame, *J. Mol. Spectrosc.* **114**, 427 (1985).

## Supplementary online information

This is a supplementary material to the paper "Autodetachment of diatomic carbon anions from long-lived high-rotation quartet states" by V. C. Schmidt *et al.* This material consists of two sections. In the first section we derive the form of the complex nonlocal operator  $F(E)$  for the case of the final  $\Pi_u$  states of the neutral molecule. The second section discusses a simplified form of this operator in a local approximation. The imaginary part of the level-shift operator  $F(E)$  is expressed in terms of the partial widths  $\Gamma_l$  that are extracted from ab-initio  $R$ -matrix calculations.

### I. NONLOCAL LEVEL-SHIFT OPERATOR $F(E)$ FOR THE NEUTRAL $\Pi$ STATES

In the nonlocal resonance model, the effective Hamiltonian that drives the decaying nuclear wave function of the negative ion can be written as [1]

$$H_{\text{eff}} = T + \frac{N(N+1)}{2\mu R^2} + V_d(R) + F(E), \quad (1)$$

where the first two terms describe the rovibrational kinetic energy,  $V_d(R)$  is the discrete-state potential curve, and  $F(E)$  denotes the complex-valued level-shift operator that contains all the couplings between the resonant and continuum states of the anion in a form of a nonlocal complex-valued interaction.

The modification of the interaction operator  $F(E)$ , for our particular case, follows the ideas presented in Ref. [2]. The necessary differences arise from the intrinsic coupling of the degenerated electronic non- $\Sigma$  states with the molecular rotations [3]. Therefore, the neutral target electronic state  $w(\tau)$  will also enter the derivation. The symbol  $\tau$  here represents, collectively, the space coordinates of the target electrons. Note that the anion state is still considered to be in the  $\Lambda = 0$  state, presently the  $C^4\Sigma_u^+$  state of  $C_2^-$ . We start from the definition of the  $F(E)$  by T.F. O'Malley [4]

$$F(E) = \langle d|QHPG_pPHQ|d\rangle, \quad (2)$$

where  $Q$  and  $P$  are the projection operators [4, 5],  $G_p = 1/P(E - H + i\epsilon)P$ , the discrete state of the anion is represented by  $|d\rangle$ , and the total Hamiltonian can be written as a sum of the nuclear kinetic energy  $T$  and of the electronic Hamiltonian  $H_{\text{el}}$ , i.e.  $H = T + H_{\text{el}}$ . The projection operator  $P$  can be expressed in the adiabatic energy-normalized eigenstates  $|\mathbf{k}^{(+)}\rangle$  of the  $PH_{\text{el}}P$  operator as [2]

$$P = \int d\mathbf{k} |\mathbf{k}^{(+)}\rangle \langle \mathbf{k}^{(+)}|. \quad (3)$$

After inserting the expansion (3) into Eq. (2) we can write

$$F(E) = \int d\mathbf{k} d\mathbf{q} \langle d|H_{\text{el}}|\mathbf{k}^{(+)}\rangle \langle \mathbf{k}^{(+)}|G_p|\mathbf{q}^{(+)}\rangle \langle \mathbf{q}^{(+)}|H_{\text{el}}|d\rangle. \quad (4)$$

The anion's background states  $|\mathbf{k}^{(+)}\rangle$  are first written in the body frame coordinates  $\mathbf{r}'$  and  $\tau$

$$\langle \mathbf{r}'|\mathbf{k}^{(+)}\rangle = \frac{1}{\sqrt{2}} \mathcal{A} \sum_{l'} \frac{1}{r'} \left[ w_{\Lambda}(\tau) \phi_{ll'}^{-\Lambda}(k, r') Y_{l-\Lambda}(\hat{\mathbf{r}}') Y_{l'-\Lambda}^*(\hat{\mathbf{k}}') + \eta w_{-\Lambda}(\tau) \phi_{ll'}^{\Lambda}(k, r') Y_{l\Lambda}(\hat{\mathbf{r}}') Y_{l'\Lambda}^*(\hat{\mathbf{k}}') \right], \quad (5)$$



where the symbol  $\mathcal{A}$  antisymmetrizes the wave function with respect to the exchange of the anion's electronic coordinates. Quantum number  $\eta$  denotes the parity of the anion state with respect to the reflection on the body-frame coordinate plane ( $x'z'$ ), that changes  $w_\Lambda$  into  $(-1)^\Lambda w_{-\Lambda}$  [6]. Recall that  $w_\Lambda$  and  $w_{-\Lambda}$  are different but degenerate for  $\Lambda \neq 0$ . For simplicity, the anionic wave function in the above equation is already assumed to possess the  $\Sigma_u^+$  symmetry as the neutral target state  $w_\Lambda$  couples only with the continuum wave function with the  $-\Lambda$  projection of its angular momentum  $l$  onto the molecular axis.

The matrix elements

$$V_{d\mathbf{k}} = \langle d|H_{\text{el}}|\mathbf{k}'^{(+)}\rangle \quad (6)$$

in Eq. (4) are first written in the body frame of reference as

$$V_{d\mathbf{k}'} = \frac{1}{\sqrt{2}} \sum_{l'} \left[ V_{dkl'}^{-\Lambda} Y_{l'-\Lambda}^*(\hat{\mathbf{k}}') + \eta V_{dkl'}^{\Lambda} Y_{l'\Lambda}^*(\hat{\mathbf{k}}') \right], \quad (7)$$

with

$$V_{dkl'}^{\Lambda} = \sum_l \langle d|H_{\text{el}}|\mathcal{A} \frac{1}{r} w_{-\Lambda} \phi_{l'}^{\Lambda} Y_{l\Lambda}\rangle. \quad (8)$$

Note that  $V_{dkl'}^{\Lambda} = V_{dkl'}^{-\Lambda}$  because both terms on the r.h.s. of Eq. (5) must be of  $\Sigma_u^+$  symmetry and the azimuthal parts of the target and continuum wave functions must cancel [3].

There is one more simplification introduced in Eq. (5) and it is omission of a sum over the target states  $w(\tau)$  accounting for the correlation and polarization effects between the ejected electron and the neutral molecule. Such a sum would slightly change the definition of  $V_{dkl'}^{\Lambda}$  since the sum would appear in the ket on the r.h.s of Eq. (8). Moreover, this sum would also enable the theory for the autodetachment decay into multiple final electronic states. However, these excited  ${}^3\Pi_u$  states do not contribute into the present study and thus they are omitted for clarity.

The  $V_{d\mathbf{k}'}$  term in (6) and (7) is a component of the level-shift operator  $F(E)$  in Eq. (4) and it depends on the momentum vector  $\mathbf{k}'$  expressed in the body frame of reference. Transformation to the unprimed coordinates attached to the laboratory frame is easily done through the Wigner D-functions as

$$V_{d\mathbf{k}} = \frac{1}{\sqrt{2}} \sum_{l'm} \left[ V_{dkl'}^{\Lambda} D_{-\Lambda m}^{l'}(\hat{\mathbf{R}}) + \eta V_{dkl'}^{-\Lambda} D_{\Lambda m}^{l'}(\hat{\mathbf{R}}) \right] Y_{l'm}^*(\hat{\mathbf{k}}), \quad (9)$$

where the unit vector  $\hat{\mathbf{R}}$  stands for the Euler angles of the diatomic molecule's orientation in the laboratory frame, i.e.  $\hat{\mathbf{R}} \equiv (0, \theta, \phi)$ .

The second term in the integral on the r.h.s of Eq. (4) represents the nuclear propagator

$$\langle \mathbf{k}^{(+)}|G_p|\mathbf{q}^{(+)}\rangle = \langle \mathbf{k}^{(+)}|(E - q^2/2 - T - V_0(R) + i\epsilon)^{-1}|\mathbf{q}^{(+)}\rangle = \langle \mathbf{k}^{(+)}|G_0(E - q^2/2)|\mathbf{q}^{(+)}\rangle, \quad (10)$$

where  $V_0(R)$  is the adiabatic potential energy curve of the neutral molecule in degenerate states  $w_\Lambda$ ,  $w_{-\Lambda}$ , and  $G_0$  is the Green's function of the neutral molecule [2, 7]. This Green's function can be expanded in the rovibrational eigenfunctions

$$Z_{\nu'N'M'}^{\Lambda\eta'}(\tau, \mathbf{R}) = \frac{1}{R} \chi_{\nu'N'}(R) X_{N'M'}^{\Lambda\eta'}(\tau, \hat{\mathbf{R}}), \quad (11)$$

where the rotational wave function of the neutral molecule, in the non- $\Sigma$  electronic state, can be written as follows [6]:

$$X_{N'M'}^{\Lambda\eta'}(\tau, \hat{\mathbf{R}}) = \left( \frac{2N'+1}{8\pi} \right)^{1/2} \left[ w_\Lambda(\tau) D_{\Lambda M'}^{N'}(\hat{\mathbf{R}}) + \eta' w_{-\Lambda}(\tau) D_{-\Lambda M'}^{N'}(\hat{\mathbf{R}}) \right]. \quad (12)$$

Similar to anion case in Eq. (5) the symbol  $\eta'$  represent the  $(x'z')$ -plane-reflection parity for the final neutral molecule. The expansion into the rotational states

$$G_0^{\Lambda\eta'}(E, \mathbf{R}, \mathbf{R}') = \sum_{N'M'} X_{N'M'}^{\Lambda\eta'}(\hat{\mathbf{R}}) \frac{1}{R} G_{0N'}(E, R, R') \frac{1}{R'} X_{N'M'}^{*\Lambda\eta'}(\hat{\mathbf{R}}'), \quad (13)$$

is then followed by the expansion of the radial Green's function into the vibrational states

$$G_{0N'}(E, R, R') = \sum_{\nu'} \frac{\chi_{\nu'}(R)\chi_{\nu'}(R')}{E - E_{\nu'N'} + i\epsilon}. \quad (14)$$

The energy levels  $E_{\nu'N'}$  are rovibrational energies of the neutral system.

All the ingredients are now prepared to evaluate the angular matrix elements of the level-shift operator  $F(E)$  defined by Eq. (4), i.e.

$$\langle Y_{N_1M_1} | F(E) | Y_{N_2M_2} \rangle = \frac{1}{RR'} \delta_{N_1N_2} \delta_{M_1M_2} f_{N_1}(E, R, R'), \quad (15)$$

where the radial component of the level-shift operator is defined as

$$f_N(E, R, R') = \sum_{lN'} \frac{1}{2} \left[ 1 + \eta'(-1)^{l+N'+N} \right] (2N' + 1) \begin{pmatrix} l & N' & N \\ \Lambda & -\Lambda & 0 \end{pmatrix}^2 \times \int dk k V_{dkl}^{\Lambda}(R) G_{0N'}(E - k^2/2, R, R') V_{dkl}^{*\Lambda}(R'). \quad (16)$$

The remaining steps just follow Refs. [2, 5]. The integration over the momentum in Eq. (16) can be done analytically because of the resolvent form (14) of  $G_{0N'}$ . The level-shift operator is by this integration split into the real and imaginary components:

$$f_N(E, R, R') = \sum_{lN'} \frac{1}{2} \left[ 1 + \eta'(-1)^{l+N'+N} \right] (2N' + 1) \begin{pmatrix} l & N' & N \\ \Lambda & -\Lambda & 0 \end{pmatrix}^2 \times \sum_{\nu'} \chi_{\nu'N'}(R) \left[ \Delta_l(E - E_{\nu'N'}, R, R') - \frac{i}{2} \Gamma_l(E - E_{\nu'N'}, R, R') \right] \chi_{\nu'N'}(R'), \quad (17)$$

where

$$\Gamma_l(\varepsilon, R, R') = 2\pi V_{dkl}^{\Lambda}(R) V_{dkl}^{*\Lambda}(R'), \quad (18)$$

$$\Delta_l(\varepsilon, R, R') = \frac{1}{2\pi} \mathcal{P} \int d\varepsilon' \frac{\Gamma_l(\varepsilon', R, R')}{\varepsilon - \varepsilon'}. \quad (19)$$

While the expressions (16) and (17) are very similar to the ones derived in Ref. [2], the factor  $g_{lN'N}^{\eta'} = (1 + \eta'(-1)^{l+N'+N})/2$  is new for the case  $\Lambda \neq 0$ . In order to understand this two-valued factor (0 or 1), we first note that due to the bosonic nuclear spin statistics of the present  $C_2^-$  system, only the odd rotational quanta  $N$  of the decaying anion are populated. Furthermore, in the studied process the  $\Sigma_u$  anion decays into the  $\Pi_u$  neutral molecule and hence the continuum electron must be of the  $\Pi_g$  symmetry, which contains only the even quanta of the ejected electron's angular momenta  $l$ . Finally, each of the final neutral rotational levels  $N'$  is nearly doubly degenerate, split by the  $\Lambda$ -doubling effect. One of the states in this pair is symmetric and the other is antisymmetric with respect to the nuclear exchange. The upper and the lower components are distinguished by the sign of  $\eta'$  [3]. Therefore the factor  $g$  simply selects only those final rotational states of

the neutral molecule, that are compatible with the nuclear spin conservation during the AD decay process.

The spherical symmetry of the level-shift operator  $F(E)$  demonstrated by Eq. (15) suggests that, in the present model, different initial rotational levels  $N$  are not coupled. However, every one of these initial levels can decay into those final states (each represented by the rotational quantum  $N'$  of the neutral molecule and ejected electron's angular momentum  $l$ ) that are allowed in the sum on the r.h.s. of Eq. (17). Furthermore, it is clear that the AD decay lifetimes into the final states are controlled by the partial widths  $\Gamma_l$ .

## II. LOCAL APPROXIMATION AND THE PARTIAL WIDTHS $\Gamma_l$

The localization of the nonlocal operator  $F(E, R, R')$  is a commonly used technique [2, 5, 7, 8] exploiting different timescales of the electronic and nuclear motions. The interaction and the centrifugal terms of the radial Schrödinger equation are written as

$$\frac{N(N+1)}{2\mu R^2} + V_d(R) + f_N(R) = \frac{N(N+1)}{2\mu R^2} + V_N^{\text{loc}}(R) - \frac{i}{2}\Gamma_N^{\text{loc}}(R), \quad (20)$$

where

$$V_N^{\text{loc}}(R) = V_0(R) + E_N^{\text{res}}(R) = V_d(R) + \Delta_N(E_N^{\text{res}}(R), R, R), \quad (21)$$

$$\Gamma_N^{\text{loc}}(R) = \Gamma_N(E_N^{\text{res}}(R), R, R). \quad (22)$$

In the present study we neglect the  $N$ -dependence of the resonance energy  $E^{\text{res}}$  as the resonance is dominantly localized in a single partial wave  $l = 2$ . In this case the term  $\Delta_l$  can be taken out of the sums in Eq. (17) and what remains, in the real part of  $f_N$ , is the resolution of identity. We estimate the error in the  $V^{\text{loc}}$  caused by this assumption in order of a few meV in the present study. Such a simplification will not be done for the imaginary part of the radial level-shift operator, because we want to explore the decay lifetimes over many orders of magnitude. Therefore, the  $\Gamma_N^{\text{loc}}$  remains as

$$\Gamma_N^{\text{loc}}(R) = \sum_{lN'\nu'} g_{lN'N}^{\nu'} (2N' + 1) \begin{pmatrix} l & N' & N \\ \Lambda & -\Lambda & 0 \end{pmatrix}^2 \Gamma_l^{\text{loc}}(R) |\chi_{\nu'N'}(R)|^2. \quad (23)$$

Because the crossing point between the anion's and neutral curve depends on both rotational quantum numbers  $N$  and  $N'$ , it would be very difficult to construct the  $R$ -dependent width function  $\Gamma_l^{\text{loc}}(R)$ . Instead, we opt to replace the  $R$ -parameterized version of the local approximation by the energy parameterization, i.e.

$$\Gamma_l^{\text{loc}}(E^{\text{res}}) = \Gamma_l(E^{\text{res}}, R(E^{\text{res}}), R(E^{\text{res}})). \quad (24)$$

Such parameterization has been previous used to characterize the two-dimensional resonant surface of the  $\text{CF}_3\text{Cl}$  molecule [9].

The partial widths were obtained at the neutral equilibrium geometry by calculations of the energy-dependent  $K$  matrices with the diatomic UK R-matrix package [10]. An example of the eigenphases, one of the ingredients to determine the partial widths, is shown in the left panel of Fig. 1. The figure demonstrates that the resonant state is strongly localized in a single eigenphase channel that should not be mistaken for the angular momentum channel. This single eigenphase channel still consists of several partial waves with a dominant  $d$ -wave contribution. The technique for extraction of the partial widths was adopted from [11, 12]. The background  $S$  matrix  $S^0$  first diagonalized

$$\underline{U}^+ \underline{S}^0 \underline{U} = e^{2i\delta^0}, \quad (25)$$

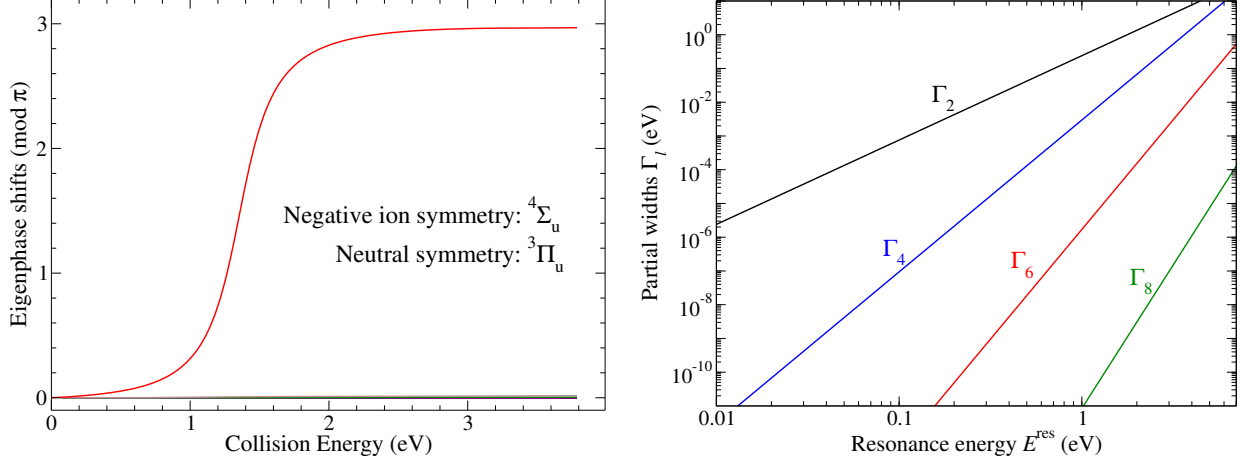


FIG. 1. Left panel: Eigenphases in the  ${}^4\Sigma_u$  symmetry as functions of the collision energy. The nuclei are fixed at the equilibrium distance  $R_0 = 2.49$  bohrs. Right panel: The energy dependence of the partial widths  $\Gamma_l^{\text{loc}}(E^{\text{res}})$ .

where  $\underline{\delta}^0$  is the diagonal matrix of the background eigenphases  $\delta_\alpha^0$ . According to Macek [13], the partial widths can be obtained by fitting the energy dependence of the eigenphases

$$2(E - E^{\text{res}}) = \sum_{\alpha} \Gamma_{\alpha} \cot [\delta_{\alpha}^0 - \delta_{\beta}(E)] \quad (26)$$

for every eigenphase  $\delta_{\beta}(E)$ . The symbol  $E^{\text{res}}$  denotes the resonance energy and  $\Gamma_{\alpha}$  describe partial widths of the decay into the eigenchannels of the background  $S$  matrix  $S^0$ . However, our LCP model requires partial widths  $\Gamma_l$  describing decays into the different partial waves of the continuum electron.

The partial widths  $\Gamma_l$  can be obtained once the full  $S$  matrix is transformed into the background eigenchannels as

$$\underline{U} \underline{A} \underline{U}^+ = \underline{S}. \quad (27)$$

While the matrix  $\underline{A}$  is diagonal for  $\underline{S}^0$ , it contains rank-1 additional resonant term for the full matrix  $\underline{S}$  [13]:

$$A_{\alpha\beta} = e^{i\delta_{\alpha}^0} \left[ \delta_{\alpha\beta} - i \frac{(\Gamma_{\alpha}\Gamma_{\beta})^{1/2}}{E - E^{\text{res}} + i\Gamma/2} \right] e^{i\delta_{\beta}^0}. \quad (28)$$

This leads directly to

$$\Gamma_l^{1/2} = \sum_{\alpha} U_{l\alpha} \Gamma_{\alpha}^{1/2}, \quad (29)$$

where  $U_{l\alpha}$  are the eigenvectors of the background  $S$  matrix  $S^0$  in Eq. (27) and the eigenchannel partial widths  $\Gamma_{\alpha}$  are obtained by fitting the formula (26).

The partial widths from the equilibrium geometry, and from the corresponding resonant energy  $E^{\text{res}}(R_{\text{eq}})$ , were then extrapolated to other geometries by an application of the threshold law  $\Gamma_l(\varepsilon) \sim \varepsilon^{l+1/2}$  [5]. The resulting energy dependence of the partial widths is shown in the right panel of Fig. 1.

While the resonant part of the anion curve was described in the previous section, the neutral and anion bound-state curves were obtained by the internally contracted Multi-Reference Configuration Interaction (MRCI) as implemented in MOLPRO 12 package of quantum-chemistry programs [14]. The wavefunctions for the MRCI method were generated by the state-averaged Multi-Configuration Self-Consistent Field (MCSCF) method with the active space of 8 and 9 electrons in 8 orbitals for  $C_2$  and  $C_2^-$ , respectively. Molecular orbitals were described by the Dunning's augmented correlation-consistent basis of quadruple-zeta quality aug-cc-pVQZ [15]. The energies of the  $A^3\Pi_u$  neutral and

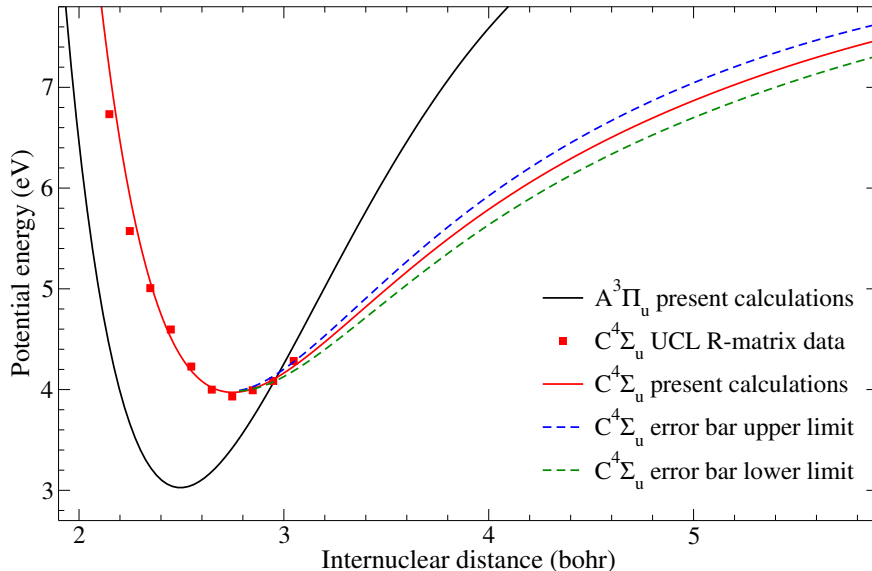


FIG. 2. Potential curves for the relevant neutral and anion states. The present calculations are shown with the full curves. Previous  $R$ -matrix calculations [16, 17] are displayed with squares. The dashed lines represent our estimate of the error bars for the present anion curve calculations.

$C^4\Sigma_u^+$  anion states, resulted from the present calculations, are displayed as the full curves in Fig. 2. These data together with the energy-dependent partial widths, shown in the right panel of Fig. 1, constitute all the electronic structure information necessary to build the effective Hamiltonian  $H_{\text{eff}}$  in Eq. (1) in the local complex approximation.

It is worth to note, that the present quartet anion curve was already studied previously by Halmová *et al.* [16, 17]. While the partial widths  $\Gamma_l$  were not analyzed in Refs. [16, 17], the resonance energy  $E^{\text{res}}$  agrees reasonably well with the present calculations (see Fig. 2). However, the major discrepancy lies in the total resonance width  $\Gamma$ . Halmová [17] reports  $\Gamma(R_{\text{eq}}) = 0.28$  eV, while in the present calculations  $\Gamma(R_{\text{eq}}) = 0.48$  eV.

Finally, in order to estimate an impact of the accuracy of our *ab initio* calculations on the final results, we introduce computational error bars in form of upper- and lower-limit anion curves as shown in Fig. 2 by the dashed lines. These curves reach maximum deviations  $\pm 170$  meV from the unperturbed  $C^4\Sigma_u$  curve at  $R = 5$  bohrs. The value of the deviation is chosen arbitrarily, as our estimate for the typical error in the correlation energy for  $\pi$ -bonded systems described by the MRCI method.

---

[1] M. Čížek, J. Horáček, and W. Domcke, Phys. Rev. A **75**, 012507 (2007).

- [2] M. Čížek and K. Houfek, in *Low-energy electron scattering from molecules, biomolecules and surfaces*, edited by P. Čárský and R. Čurík (CRC Press, Boca Raton, 2012) 1st ed., Chap. 4, pp. 91–125.
- [3] G. Herzberg, *Molecular Spectra and Molecular Structure I. Spectra of Diatomic Molecules* (D. Van Nostrand Company, Inc., New York, 1950).
- [4] T. F. O'Malley, Phys. Rev. **150**, 14 (1966).
- [5] W. Domcke, Phys. Rep. **208**, 97 (1991).
- [6] E. S. Chang and U. Fano, Phys. Rev. A **6**, 173 (1972).
- [7] R. J. Bieniek, Phys. Rev. A **18**, 392 (1978).
- [8] D. J. Haxton, C. W. McCurdy, and T. N. Rescigno, Phys. Rev. A **75**, 012710 (2007).
- [9] M. Tarana, P. Wielgus, S. Roszak, and I. I. Fabrikant, Phys. Rev. A **79**, 052712 (2009).
- [10] L. A. Morgan, C. J. Gillan, J. Tennyson, and X. S. Chen, J. Phys. B: Atom. Molec. Phys. **30**, 4087 (1997).
- [11] A. U. Hazi, Phys. Rev. A **19**, 920 (1979).
- [12] D. J. Haxton, C. W. McCurdy, and T. N. Rescigno, Phys. Rev. A **73**, 062724 (2006).
- [13] J. Macek, Phys. Rev. A **2**, 1101 (1970).
- [14] H. J. Werner, P. J. Knowles, R. Lindh, F. R. Knizia, F. R. Manby, M. Schütz, and Others, MOLPRO, version 2012.1, a package of ab initio programs (2012).
- [15] T. H. Dunning, J. Chem. Phys. **90**, 1007 (1989).
- [16] G. Halmová, J. D. Gorfinkiel, and J. Tennyson, J. Phys. B: Atom. Molec. Phys. **39**, 2849 (2006).
- [17] G. Halmová, *R-matrix calculations of electron-molecule collisions with  $C_2$  and  $C_2^-$* , Ph.D. thesis, University College London (2008).